Experimental and Theoretical Studies of MCF_3^+ (M = Fe and Co): Reactivities, Structures, and Potential Energy Surface for C−F Activation

Quan Chen*,† and Ben S. Freiser‡

H. C. Brown Laboratory of Chemistry, Purdue University, West Lafayette, Indiana 47907

Received: February 27, 1998

The gas-phase reactions of $FeCF_3^+$ and $CoCF_3^+$ with a series of small alkanes and alkenes were studied by Fourier transform ion cyclotron resonance (FTICR) mass spectrometry. These ions, which are generated from the reactions of the bare metal ions with CF_3I, both react with alkanes larger than ethane and with small alkenes primarily by CF_2 displacement reactions. Hydride abstraction is also observed in some cases. Collision-induced dissociation and ion−molecule reactions indicate that the structure of MCF_3^+ (M = Fe, Co) is an ion−dipole complex, $FM^+\cdots F_2C$, involving C−F activation. A good fit of pseudo-first-order kinetics is obtained for the reactions of $FeCF_3^+$ and $CoCF_3^+$ with the above selected hydrocarbons. The reaction rates of $FeCF_3^+$ and $CoCF_3^+$ with the alkanes increase dramatically with the length of the alkane chain. The C−F activation mechanism of Fe^+ or Co^+ with the CF_3 ligand was also investigated theoretically. The potential energy surface (PES) of the $[Fe, C, F_3]^+$ system and the local minima of the $[Co, C, F_3]^+$ system are examined by density functional calculations. For the iron system, three local minima are detected including the intact trifluoromethyl isomer, Fe^+-CF_3, the inserted fluoro−difluorocarbene isomer, F_2C-Fe^+-F, and the ion−dipole complex, $FCF\cdots Fe^+-F$. Two transition-state structures connecting the above minima are also found. The PES of $[Fe, C, F_3]^+$ indicates a unique mechanism in which C−F insertion takes place first with a large activation barrier of 6.4 kcal/mol, followed by rotation of the CF_2 unit to the final $FCF\cdots Fe^+-F$ structure with an activation barrier of 2.4 kcal/mol. Three similar minima are also detected for $CoCF_3^+$.

Introduction

The effect of ligands on the reactivity of metal ions is a topic of great current interest in gas-phase organometallic ion chemistry.[1] Previous studies have shown that the reactivity of a gas-phase metal ion is dramatically altered by the addition of a ligand. While M^+ (M = Fe, Co, Ni) reacts with alkanes predominantly by oxidative insertion into C−C bonds,[2−6] for example, C−H insertion occurs exclusively in the reactions of MCH_3^+ (M = Fe, Co),[7] MO^+ (M = Fe, Co),[8−10] and MS^+ (M = Fe, Co, Ni).[11] Migratory insertions and olefin metathesis are also observed.[12] The overall reactivity of a metal ion can be either increased or decreased by the presence of a ligand.

CF_3 radical, the fluorine-containing analog of methyl radical, is a highly stable functional group found in many hydrofluorocarbons (HFCs).[13,14] Little is known, however, about the ligand effect of CF_3 on bare metal ions. The ability of the fluorine atom to function as a σ acceptor arises as a result of its high electronegativity. On the other hand, fluorine atom is also a good π electron donor to carbon π systems owing to the match of its lone-pair 2p orbital to that of carbon.[15] Thus, the effect of fluorine substitution is the combination of inductively withdrawing and π donating.

The structures of alkyl radicals often change dramatically upon fluorine substitution. The results from UV, IR, PES, and ESR spectroscopies and high-level ab initio calculations indicate that methyl radical has a planar structure, for example, while fluoromethyl radicals become more pyramidal with increasing numbers of fluorine atoms. In particular trifluoromethyl has a tetrahedral structure.[16] Halle, Armentrout, and Beauchamp have studied fluorine substituent effects on carbene stability and the metathesis reactions of fluorinated olefins with $NiCH_2^+$ and $NiCF_2^+$.[17] One of the interesting findings was that $D^0(Ni^+-CF_2) = 47 \pm 7$ kcal/mol, which is substantially lower than $D^0(Ni^+-CH_2) = 86 \pm 6$ kcal/mol.

C−F bond activation by metal centers in solution,[18−21] on surfaces[22] and in the gas phase[23−28] is a topic of great interest owing to the great strength of the C−F bond and the high electronegativity of fluorine. In solution, aryl and alkyl C−F bond activation has been achieved in catalytic processes using both electron-deficient and electron-rich transition-metal complexes.[18] Electron-deficient metals include lanthanides, actinides, and groups III−V transition metals with partially filled d orbitals. Defluorination is achieved as a result of the coordinatively unsaturated metal center and the strong metal−fluoride bond.[18] For example, Burns and Andersen have observed that $Yb(C_5Me_5)_2$ can cleave C−F bonds in C_6F_6, CF_2CH_2, and C_2F_4 to form $(C_5Me_5)_4Yb_2(\mu\text{-}F)$, which is characterized by X-ray diffraction to be a $Yb^{II}-F-Yb^{III}$ mixed-valence complex.[19] The majority of the C−F activation reactions, however, involve electron-rich d^n ($n \geq 6$) transition-metal centers and occur via oxidative addition.[18a] For example, Aizenberg and Milstein have reported on a homogeneous transition-metal-catalyzed aryl C−F activation by rhodium trimethylphosphine complexes under mild conditions in the presence of a base such as Et_3N.[20] Richmond and co-workers have demonstrated that perfluorodecalin can be defluorinated with cobaltocene in toluene solution in the presence of $Li[O_3SCF_3]$ at room temperature yielding cobaltocenium fluoride.[18b] Burdeniuc and Crabtree have reported the successful use of decamethylferrocene as a photosensitizer and a one-electron reducing agent

* Corresponding author.

† Present address: Hospital Product Division, Abbott Laboratories, D-971, AP4/2, 100 Abbott Park Road, Abbott Park, IL 60064-3500.

‡ Deceased on December 30, 1997.

S1089-5639(98)01336-X CCC: $15.00
Published on Web 04/15/1998

to activate C−F bonds in perfluoromethylcyclohexane by photoinduced charge transfer.[21]

Cooks and co-workers have observed single and multiple fluorine abstractions by low-energy (<100 eV) transition-metal ions (M = Ti, Cr, Fe, Mo, W) and groups IIIA-VIIA ions impinging upon fluorinated self-assembled monolayer surfaces.[22] The mechanism they proposed involves fluorine abstraction via formation of a short-lived collision complex, which is formed by multiple collisions between the projectile and a small group of atoms near the surface. A direct oxidative addition mechanism was favored over an electron-transfer process since the reaction occurred at energies far below the chemical sputtering threshold.[22a]

In the gas-phase, C−F bond activation by metal centers is still a relatively unexplored area. The first case of C−F activation was reported by Ridge and co-workers in the reaction of Fe^+ with fluorobenzene studied using an ICR spectrometer.[23] The primary product ion observed is $Fe(C_6H_4)^+$, generated by the loss of HF, which can then react further with fluorobenzene by loss of HF forming an iron diphenylene complex.[23] Bjarnason and Taylor have reported similar findings in an expanded study on the reactions of Fe^+ with other phenyl halides.[24] Cooks and co-workers reported the gas-phase ion/molecule reactions of $W(CO)_6^{\bullet+}$ and perfluorohexane yielding $[W(CO)_6{\bullet}C_6F_{13}]^+$, which upon CID generates WF_n^+ (n = 1−5) product ions.[25] Schwarz and colleagues observed the C−F activation product FeF^+ by reacting FeO^+ with hexafluorobenzene in an FTICR mass spectrometer.[27] In a recent paper, Schwarz and co-workers discussed the reactivity of bare Ln^+ (Ln = La−Lu) with various fluorinated hydrocarbons such as CF_4, CHF_3, CH_3F, C_2F_6, and C_6F_6. C−F insertion was found to be generally observed in these reactions, and they proposed a mechanism involving a $[Ln^{2+}{\cdots}F^-{\cdots}R]$-type intermediate, formed by single electron transfer from Ln^+ to the fluorine atom upon the coordination of R−F to Ln^+.[28] This intermediate then forms LnF^+ by C−F cleavage. Schwarz and co-workers also demonstrated C−F activation by bare Ca^+ with organic fluorides, which generates CaF^+ and the corresponding radicals. The theoretical calculations indicate a tight transition structure and a similar mechanism that includes electron transfer, followed by metal−fluorine bond formation.[29]

In a previous preliminary study, we reported the first case of C−F activation by bare Co^+ in the reaction of Co^+ with CF_3I in the gas phase.[30] As an extension of that work, we present here the results of an experimental study of the gas-phase reactions of MCF_3^+ (M = Fe, Co) with small hydrocarbons, together with a comprehensive theoretical investigation of the C−F activation mechanism, in which the minima and saddle points on the $[M, C, F_3]^+$ potential energy surfaces (PES) are obtained using density functional calculations. The results from the theoretical calculations are also used to explain the nature of the chemical bonding of both species, to estimate the bond energies, and to discuss the thermochemistry of related reactions.

Experimental Section

All of the experiments were performed with a Nicolet (now Finnigan FT/MS, Madison, WI) prototype FTMS-1000 Fourier transform mass spectrometer, equipped with a 5.2 cm cubic trapping cell situated between the poles of a Walker Scientific 15-in. electromagnet, which was maintained at 1 T.[31] The cell has two 80% transmittance stainless steel mesh transmitter plates, and one of them holds various metal targets. Laser desorption ionization was used to generate Fe^+ or Co^+ from the pure metal foil by focusing the fundamental wavelength (1064 nm) of a Quanta-Ray Nd:YAG laser on the metal target.[32]

Chemicals, obtained commercially in high purity, were used as supplied except for multiple freeze−pump−thaw cycles to remove the noncondensable gases. Argon was present at a static background pressure of $\sim 1.0 \times 10^{-5}$ torr, serving as a cooling gas to thermalize the ions prior to reactions, and at a total pressure of $\sim 2.0 \times 10^{-5}$ Torr as the collision gas in collision-induced dissociation (CID)[33] and sustained off-resonance irradiation (SORI)[34] experiments. The cell pressure was monitored with a Bayard-Alpert ionization gauge.

In analogy to the synthesis of $CoCH_3^+$ from CH_3I,[35] laser-desorbed M^+ (M = Fe, Co) was reacted with trifluoromethyl iodide, which was pulsed into the cell via a General Valve Series 9 solenoid pulsed valve.[36] The major products were found to be MI^+ (70−85%) and CF_2I^+ (10−20%). The minor MCF_3^+ (M = Fe, Co) product ion (5−10%) was then isolated by using swept double-resonance ejection techniques[37] and cooled 400 ms prior to further reaction. Alkane and alkene neutrals were introduced into the cell by a second pulsed valve to a maximum pressure of $\sim 1.0 \times 10^{-6}$ Torr to react with $FeCF_3^+$ or $CoCF_3^+$. The primary product ion structures were investigated by collision-induced dissociation (CID), sustained off-resonance irradiation (SORI), and ion−molecule reactions. The maximum translational energy acquired during CID by the ions is given in the laboratory frame and was calculated using the following equation applicable to a cubic cell[38]

$$E_{tr}(\max) = \frac{E_{RF}^2 q^2 t^2}{16 M_{ion}}$$

where E_{RF} is the electric-field amplitude, t is the duration of the electric field applied, q is the charge of the ion, and M_{ion} is the mass of the ion to be excited. The center-of-mass energy of the parent ion, corresponding to the maximum internal energy that can be converted from the translational energy after undergoing a single collision with the target gas, is calculated by the following equation

$$E_{cm} = \frac{M_{target}}{M_{target} + M_{ion}} E_{tr}(\max)$$

where M_{target} is the mass of the collision gas, which is argon in this case. All of the energies mentioned are in the center-of-mass frame. Under the time and pressure conditions used in the experiment, however, CID is a multiple-collision process and, thus, the actual internal energy of the ion can be higher than E_{cm}.

For the kinetics study, the alkane and alkene neutrals were introduced into the cell through a Varian leak valve. The pressure of the neutral reagent was kept at $\sim 2.5 \times 10^{-7}$ Torr and Ar was used as the cooling gas with a total pressure of $\sim 1.0 \times 10^{-5}$ Torr. The pressure of the alkane neutral was measured using standard procedures for calibrating the ion gauge for the sensitivity toward the alkane.[39] The reaction time was varied between 200 ms and 5 s to obtain the kinetics plots for the reactions of $FeCF_3^+$ and $CoCF_3^+$ with the hydrocarbons. The uncertainty in the pressure introduces an error of ±30% into the measurement of the absolute reaction rate constants, while the relative reaction rate constants are more reliable.

Computations

All of the calculations were performed using DFT with Becke3LYP for the exchange correlation functional.[40] This functional has three fitted parameters and includes a Hartree−Fock exchange term. Of course this functional is not exact[41]

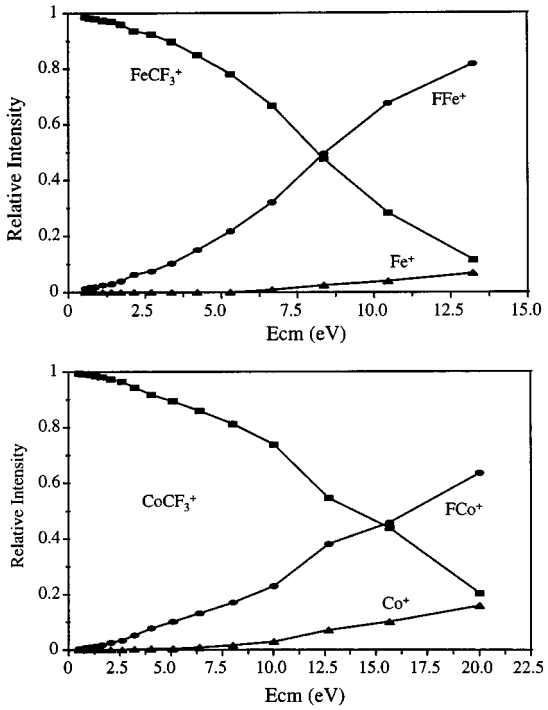

Figure 1. Relative ion intensity versus center-of-mass energy for CID of $FeCF_3^+$ and $CoCF_3^+$. Duration of the excitation RF pulse is 300 μs followed by a 50 ms time delay.

but gives relatively accurate results for bond dissociation energies and geometries of transition-metal compounds.[42] For carbon and fluorine, we use 6-311+G* basis sets. For Fe and Co, we use the Wachters−Hay all-electron basis set,[43] with a (611111111|51111|311) → [9s 5p 3d] contraction. All stationary points were characterized as minima or first-order transition structures by evaluating the frequencies and normal modes by using analytical first derivatives and the computed force constant matrix. Corrections for zero-point energies have been taken into account, and different spin configurations have also been considered, including the ^{4}F and ^{6}D states for Fe^+ and the ^{3}F and ^{5}F states for Co^+. Spin contamination was small in all of the calculations, and the deviation of $\langle S^2 \rangle$ is less than 3%. The errors introduced by calculations for the relative energies for different isomers are estimated to be ±5 kcal/mol on the basis of our and others' experiences.[44,45] All of the calculations were performed with the Gaussian 94 program package[46] at the Purdue University Computer Center (PUCC) and on a Silicon Graphics O2 workstation in our laboratory.

Results and Discussion

1. Structures of MCF_3^+ (M = Fe, Co). The structures of $FeCF_3^+$ and $CoCF_3^+$ ions were studied qualitatively by collision-induced dissociation (CID) and sustained off-resonance irradiation (SORI). Previous studies have shown that CID of $FeCH_3^+$ and $CoCH_3^+$ yield Fe^+ and Co^+, exclusively, by loss of intact CH_3.[7] Similarly, $FeCF_3^+$ and $CoCF_3^+$ were assumed to have trifluoromethyl−M^+ structures**.** However, both CID and SORI yield difluorocarbene loss as the major fragmentation pathway over the range of kinetic energies studied (1−23 eV for CID and 0.7−1 eV for SORI), indicative of a possible fluoro−M^+−difluorocarbene structure. Energy-resolved CID plots of $FeCF_3^+$ and $CoCF_3^+$ are illustrated in Figure 1.

The fluoro−M^+−difluorocarbene structure of MCF_3^+ was further confirmed by the reactions of $FeCF_3^+$ and $CoCF_3^+$ with ligands such alkanes, alkenes, benzene, water and acetonitrile, which all result in a predominant CF_2 displacement product, F−Fe^+−L and F−Co^+−L, respectively. As the polarizability of the ligand increases, the displacement reaction rate increases dramatically. These results indicate that CF_3 is not an intact ligand and that the CF_2 group is bound weakly to Fe^+ and Co^+, in contrast to the M^+−methyl structure of MCH_3^+ (M = Fe and Co).[7] The details of the reactions of $FeCF_3^+$ and $CoCF_3^+$ with various ligands will be discussed later, as well as the density functional calculations, which also indicate that MCF_3^+ (M = Fe, Co) is a [$FM^+\cdots F_2C$] ion−dipole complex.

2. The Reactions of $FeCF_3^+$ and $CoCF_3^+$ with Alkanes. Like M^+ and MCH_3^+ (M = Fe, Co), no reactions were observed for $FeCF_3^+$ and $CoCF_3^+$ with either methane or ethane. However, both $FeCF_3^+$ and $CoCF_3^+$ react with alkanes larger than ethane primarily by CF_2 displacement, and also by hydride abstraction in some cases, Table 1. The branching ratios of primary product ions are reproducible to within ±10%. For comparison, $FeCH_3^+$ is completely unreactive with alkanes, while $CoCH_3^+$ reacts with alkanes larger than ethane by initial C−H insertion, followed by CH_4 and H_2 loss to yield the Co-(allyl)$^+$ species. Thus, the reactivity of $FeCF_3^+$ increases dramatically upon fluorine substitution on the methyl ligand.

Propane. $FeCF_3^+$ reacts slowly with propane to produce only the condensation product, $FeCF_3(C_3H_8)^+$. Upon CID (3−5 eV) or SORI (0.6−1.4 eV) this ion regenerates $FeCF_3^+$, implying $D^0(FFe^+-F_2C) > D^0(FFe^+-C_3H_8) \approx D^0(Fe^+-C_3H_8) = 17.9 \pm 1$ kcal/mol,[47] a rough but useful estimate. On the other hand, the only primary product from the reaction of $CoCF_3^+$ with propane is the CF_2 displacement product, $FCo(C_3H_8)^+$, which fragments to FCo^+ upon CID, exclusively. This suggests that $D^0(FCo^+-F_2C) < D^0(FCo^+-C_3H_8) \approx D^0(Co^+-C_3H_8) = 30.9 \pm 1.4$ kcal/mol,[48] again only a rough estimate.

n-Butane and Isobutane. $FeCF_3^+$ reacts with *n*-butane yielding two products, reactions 1 and 2. CID of the major product, $FFe(C_4H_{10})^+$, yields FFe^+, exclusively, via loss of intact C_4H_{10}. The reaction of $FeCF_3^+$ with isobutane is similar to that with *n*-butane, giving two reaction products by CF_2 displacement (90%) and hydride abstraction (10%).

$$FeCF_3^+ + n\text{-}C_4H_{10} \xrightarrow{92\%} F\text{-}Fe^+\text{-}(C_4H_{10}) + CF_2 \quad (1)$$

$$\xrightarrow{8\%} C_4H_9^+ + FeCF_3H \quad (2)$$

$CoCF_3^+$ reacts with *n*-butane yielding three products, reactions 3−5. $CoCF_3(C_3H_6)^+$ is likely generated from terminal

$$CoCF_3^+ + n\text{-}C_4H_{10} \xrightarrow{75\%} CoCF_3(C_3H_6)^+ + CH_4 \quad (3)$$

$$\xrightarrow{18\%} CoF(C_4H_{10})^+ + CF_2 \quad (4)$$

$$\xrightarrow{7\%} CoCF_3(C_4H_{10})^+ \quad (5)$$

C−C insertion followed by β-H transfer and, ultimately, CH_4 loss. This ion in turn gives a dehydrogenation product upon CID at about 3 eV, $CoCF_3(C_3H_4)^+$, and yields FCo^+ as the major product at higher collision energies. The CF_2 displacement product, $CoF(C_4H_{10})^+$, gives FCo^+ exclusively upon CID, suggesting that C_4H_{10} remains intact in the complex. CID of the condensation product, $Co(CF_3)(C_4H_{10})^+$, yields $CoCF_3^+$ predominantly at low energies, 2−4 eV, and FCo^+ at higher energies, presumably from subsequent fragmentation of $CoCF_3^+$. The above results imply that $D^0(FCo^+-F_2C) > D^0(FFe^+-C_4H_{10})$. No hydride abstraction product is observed, in contrast to the reaction of $FeCF_3^+$ with *n*-butane. Surprisingly then, in

TABLE 1: Percentage Abundance of Primary Products Observed in the Reactions of $FeCF_3^+$ and $CoCF_3^+$ with Various Alkanes

	$FeCF_3^+$			$CoCF_3^+$		
alkanes	neutral lost	products	%	neutral lost	products	%
CH_4		no rxn			no rxn	
C_2H_6		no rxn			no rxn	
C_3H_8		$FeCF_3(C_3H_8)^+$	100	CF_2	$CoF(C_3H_8)^+$	100
n-C_4H_{10}	CF_2	$FeF(C_4H_{10})^+$	92	CH_4	$CoCF_3(C_3H_6)^+$	75
	($FeCF_3H$)	$C_4H_9^+$	8	CF_2	$CoF(C_4H_{10})^+$	18
					$CoCF_3(C_4H_{10})^+$	7
i-C_4H_{10}	CF_2	$FeF(C_4H_{10})^+$	90	($CoCF_3H$)	$C_4H_9^+$	70
	($FeCF_3H$)	$C_4H_9^+$	10	CH_4	$CoCF_3(C_3H_6)^+$	18
				CF_2	$CoF(C_4H_{10})^+$	12
n-C_5H_{12}	CF_2	$FeF(C_5H_{12})^+$	100	CF_2	$CoF(C_5H_{12})^+$	100
i-C_5H_{12}	CF_2	$FeF(C_5H_{12})^+$	100	($CoCF_3H$)	$C_5H_{11}^+$	71
				CF_2	$CoF(C_5H_{12})^+$	29
neo-C_5H_{12}	CF_2	$FeF(C_5H_{12})^+$	100	CF_2	$CoF(C_5H_{12})^+$	71
					$CoCF_3(C_5H_{12})^+$	29
n-C_6H_{14}	CF_2	$FeF(C_6H_{14})^+$	100	CF_2	$CoF(C_6H_{14})^+$	100
n-C_7H_{16}	CF_2	$FeF(C_7H_{16})^+$	100	CF_2	$CoF(C_7H_{16})^+$	100

the reaction of $CoCF_3^+$ with isobutane, the hydride abstraction product *i*-$C_4H_9^+$ is dominant, as shown in reactions 6-8. Similarly, $CoCH_3^+$ was also reported to abstract a hydride from alkanes larger than ethane forming $C_nH_{2n+1}^+$, with the exception of neopentane.[7a]

$$CoCF_3^+ + i\text{-}C_4H_{10} \xrightarrow{70\%} i\text{-}C_4H_9^+ + CoCF_3H \quad (6)$$

$$\xrightarrow{18\%} CoCF_3(C_3H_6)^+ + CH_4 \quad (7)$$

$$\xrightarrow{12\%} CoF(C_4H_{10})^+ + CF_2 \quad (8)$$

n-Pentane, Isopentane, and Neopentane. $FeCF_3^+$ reacts with C_5 alkanes yielding CF_2 displacement products, exclusively, which fragment to give FFe^+ upon CID or SORI. However, for $CoCF_3^+$, in addition to the CF_2 displacement product, the hydride abstraction product *i*-$C_5H_{11}^+$ from the reaction with isopentane and the condensation product $CoCF_3(C_5H_{12})^+$ from the neopentane reaction are also seen, reactions 9−12. CID of *i*-$C_5H_{11}^+$, a stable carbocation obtained from the isopentane reaction, generates $C_3H_7^+$ by the loss of C_2H_4. The fact that $CoCF_3^+$ does not abstract hydride from neopentane implies that hydride abstraction cannot occur from a primary carbon. Upon CID at lower energies (∼2 eV) and SORI, $CoCF_3(C_5H_{12})^+$, obtained from the neopentane reaction, yields $CoCF_3^+$ as the major fragment, suggesting that $D^0(FCo^+-F_2C) > D^0(FCo^+-C_5H_{12})$. Figure 2 illustrates typical spectra from the reaction of $FeCF_3^+$ with *n*-pentane.

$$CoCF_3^+ + i\text{-}C_5H_{12} \xrightarrow{71\%} i\text{-}C_5H_{11}^+ + CoCF_3H \quad (9)$$

$$\xrightarrow{29\%} CoF(C_5H_{12})^+ + CF_2 \quad (10)$$

$$CoCF_3^+ + neo\text{-}C_5H_{12} \xrightarrow{71\%} CoF(C_5H_{12})^+ + CF_2 \quad (11)$$

$$\xrightarrow{29\%} CoCF_3(C_5H_{12})^+ \quad (12)$$

n-Hexane and n-Heptane. The reactions of both $FeCF_3^+$ and $CoCF_3^+$ with these longer linear alkanes generate CF_2 displacement products, exclusively. CID or SORI of the product ions gives FM^+ as the only fragmentation pathway. As the length of the alkane chain increases, the reaction rate between MCF_3^+ and the alkane increases significantly.

3. Kinetics Studies of $FeCF_3^+$ and $CoCF_3^+$ with Alkanes. Pseudo-first-order kinetics are observed for the reactions of

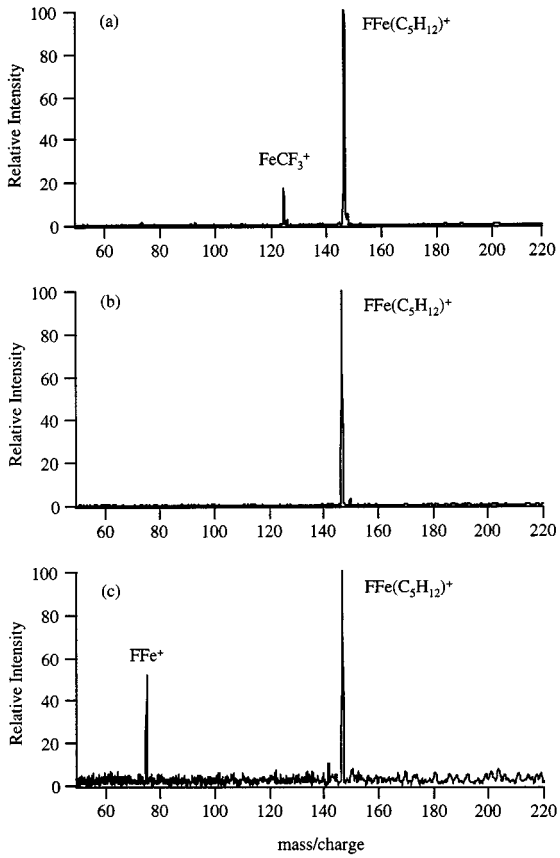

Figure 2. (a) Reaction of $FeCF_3^+$ with *n*-pentane that was pulsed into the cell at a maximum presence of $\sim 1.0 \times 10^{-6}$ Torr, 200 ms; (b) Isolation of product ion, $FFe(C_5H_{12})^+$; (c) CID of $FFe(C_5H_{12})^+$. Duration of the excitation RF pulse is 300 μs followed by a 50 ms time delay.

$FeCF_3^+$ and $CoCF_3^+$ with propane, *n*-butane, *n*-pentane, *n*-hexane, and *n*-heptane. For example, the kinetics plots of both ions with *n*-heptane are shown in Figure 3. [A] is reactant ion intensity after time *t*, and $[A]_0$ is obtained by summing the intensities of the reactant ion and product ions at each time. The slopes of the pseudo-first-order plots are used with the calibrated reactant pressure to obtain the observed rate constants, k_{obs}. The Langevin rate constants, k_L, are also calculated to determine reaction efficiencies.[49] The reaction efficiency can be obtained by taking the ratio of k_{obs} and k_L. The values obtained for k_{obs}, k_L, and the reaction efficiencies are listed in Table 2. The pseudo-first-order kinetics observed for the above

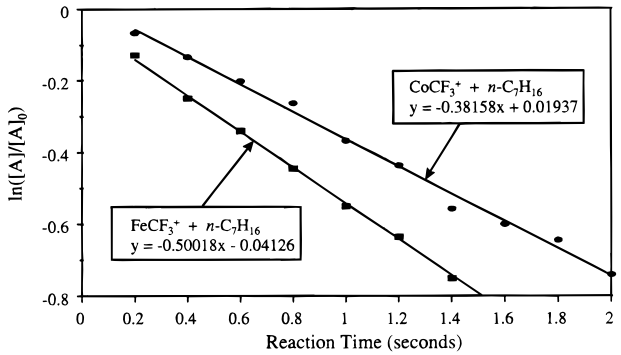

Figure 3. Pseudo-first-order plot of the reaction of $FeCF_3^+$ and $CoCF_3^+$ with *n*-heptane leaked into the cell at $\sim 2.5 \times 10^{-7}$ Torr.

reactions indicate, but not unequivocally, that the $FeCF_3^+$ and $CoCF_3^+$ species are thermalized and consist each of one isomeric structure. As the length of the alkane chain increases, the reaction rate between $FeCF_3^+$ or $CoCF_3^+$ and the alkane dramatically increases owing to the increasing polarizability of the alkanes. These results are consistent with a weakly bound ion−dipole complex of $FM^+\cdots F_2C$. A comparison of the reaction rates indicates that the reactions of $FeCF_3^+$ are generally faster than those of $CoCF_3^+$ by factors of 1.3−7.7.

4. The Reactions of $FeCF_3^+$ and $CoCF_3^+$ with Alkenes. The primary reaction products of $FeCF_3^+$ and $CoCF_3^+$ with selected alkenes are summarized in Table 3. The reaction of $FeCF_3^+$ with various alkenes results in the formation of the CF_2 displacement products, $FFe(C_nH_{2n})^+$, exclusively. While $FeCH_3^+$ is unreactive with ethene, $FeCF_3^+$ reacts with ethene yielding $FFe(C_2H_4)^+$, suggesting that $D^0(FFe^+-F_2C) < D^0(FFe^+-C_2H_4) \approx D^0(Fe^+-C_2H_4) = 34 \pm 2$ kcal/mol.[50] This reaction, coupled with the reaction of $FeCF_3^+$ with propane, bracket $D^0(FFe^+-F_2C)$ approximately in the range of $(17.9 \pm 1.0)-(34 \pm 2)$ kcal/mol. Loss of C_2H_4 to generate FFe^+ is the only fragmentation process observed in the CID of $FFe(C_2H_4)^+$. No secondary reaction was observed owing to the strong bonding between Fe^+ and F, making displacement of F by C_2H_4 impossible. CID of the product ion from the reaction with propene, $FFe(C_3H_6)^+$, yielded loss of HF at low collision energies, while at higher collision energies loss of C_3H_6 is also observed. Loss of HF, corresponding to Fe^+−allyl complex, indicates that the allylic hydrogen undergoes a rearrangement at lower collision energies. Similar reaction products and CID results are observed for the reactions of $FeCF_3^+$ with 1-butene, isobutene, and *cis*-2-butene. The reaction of $FeCF_3^+$ with 1,3-butadiene also results in exclusive formation of the CF_2 displacement product, $FFe(C_4H_6)^+$, which yields $FeC_4H_5^+$ and FFe^+ upon CID at low collision energies and higher collision energies, respectively. For comparison, $FeCH_3^+$ reacts with propene, isobutene, 1-butene, *cis*-2-butene, and 1,3-butadiene, respectively, yielding an activated π-allyl complex by initial elimination of methane.

The reactions of $CoCF_3^+$ with selected alkenes are similar to those of $FeCF_3^+$. In addition to the CF_2 displacement product, the minor product ions (<10%) from the reactions with propene, isobutene, and 1-butene proceed from alkene hydrogen abstraction followed by CF_3H elimination, similar to the CH_4 elimination from $CoCH_3^+$ reactions with alkenes larger than propene. CID of the major product ions formed by CF_2 displacement gives loss of HF at low collision energies, while at higher collision energies loss of C_nH_{2n} is also observed. Figure 4 shows typical spectra for the reaction of $CoCF_3^+$ with 2-methylpropene.

5. Kinetics Studies of $FeCF_3^+$ and $CoCF_3^+$ with Alkenes. Pseudo-first-order kinetics are, once again, observed for the reactions of $FeCF_3^+$ and $CoCF_3^+$ with ethene, propene, and 1-butene. The slopes of the pseudo-first-order plots are used with the calibrated reactant pressures to obtain the observed rate constants, k_{obs}. The reaction efficiency is obtained by taking the ratio of k_{obs} and k_L. The estimated rate constants k_{obs}, k_L, and the reaction efficiencies are tabulated in Table 4. A good fit of first-order kinetics indicates, once again, that $FeCF_3^+$ and $CoCF_3^+$ species are likely thermalized and consist of one isomeric structure. As the length of the alkene chain increases, the reaction rate between $FeCF_3^+$ or $CoCF_3^+$ and the alkene increases. These results are again consistent with the weakly bound ion−dipole complex, $FM^+\cdots F_2C$. The comparison of the reaction rates shows that the reactions of $FeCF_3^+$ with alkenes are relatively faster than that of $CoCF_3^+$ by factors of 5−6, implying that $D^0(FFe^+-CF_2)$ is possibly lower than $D^0(FCo^+-CF_2)$.

6. Ion−Molecule Reactions with Benzene, Acetonitrile, and Water. The ion−molecule reactions of $FeCF_3^+$ and $CoCF_3^+$ with benzene, acetonitrile, and H_2O were also studied. The reactions with benzene and acetonitrile yield exclusive CF_2 displacement products, $FM(C_6H_6)^+$ and $FM(CH_3CN)^+$, respectively, which generate FM^+ upon CID or SORI. Figure 5 shows typical mass spectra of $CoCF_3^+$ with acetonitrile. While the reaction with water also generates a CF_2 displacement product, FM^+-H_2O, a secondary product, $FM^+-(H_2O)_2$, is also observed in contrast to the reactions of other ligands.

7. C−F Activation Mechanism: Potential Energy Surface for Fe^+ with $CF_3^\bullet$. Recently, density functional theory (DFT) has attracted a great deal of attention owing to its two distinct advantages: its inclusion of Hartree−Fock exchange corrections in basic formulas and its computational efficiencies.[42,51] DFT has been applied to the calculations of various open-shell transition metal species yielding accurate bond energies and geometries.[52−56] For example, Koch and co-workers have reported the potential energy surfaces for the reactions of Fe^+ and Co^+ with ethane in the activation of C−C bonds and C−H bonds.[55−56] Bauschlicher and co-workers have obtained Becke3LYP binding energies for MCH_2^+ systems involving first row transition metals, which are in excellent agreement with the experimental values.[53] In the course of this study, we employed Becke3LYP to investigate the potential energy surface for the interaction of Fe^+ with CF_3, with a particular focus on the C−F bond activation mechanism.

For the $[Fe, C, F_3]^+$ system, the optimized geometries of the relevant stationary points on the potential energy surface are shown in Figure 6, and the potential energy surface for Fe^+ and $CF_3^\bullet$ is given in Figure 7. Initially, $Fe^+(^6D)$ and $CF_3^\bullet$ approach each other to form an intact $Fe(CF_3)^+$ complex **1**. The $^5A''$ ground state of **1** has C_{3v} symmetry and is computed to be 41.4 kcal/mol more stable than the $Fe^+(^6D) + CF_3^\bullet$ entrance channel. The CF_3 group in the complex remains almost unchanged compared to the free CF_3 radical.[57] The C−F bond distance and F−C−F angle are calculated at 1.331 Å and 108.8°, respectively, compared to 1.323 Å and 111.3° in free CF_3.[57] The Fe−C bond length of 2.054 Å is about 0.039 Å longer than that of Fe^+-CH_3 calculated by Bauschlicher and co-workers using the modified coupled pair functional (MCPF) approach.[58] Even though these two calculations were performed with different functionals at different levels, the calculated values provide a useful comparison. The corresponding $^3A''$ state of **1** is less stable than the $^5A''$ state by 22.9 kcal/mol. The Mulliken population analysis for the ground state gives the charge distribution as the following: $q = +1.121$ for Fe and $q = -0.121$ for the CF_3 group. Although there is a covalent bond

TABLE 2: Pseudo-First-Order Rate Constants and Calculated Reaction Efficiencies for the Reactions of $FeCF_3^+$ and $CoCF_3^+$ with Linear Alkanes[a]

	$FeCF_3^+$			$CoCF_3^+$		
reagent	k_{obs}	k_L	reaction efficiency (%)	k_{obs}	k_L	reaction efficiency (%)
propane	3.7×10^{-12}	1.0×10^{-9}	0.4	1.3×10^{-12}	1.0×10^{-9}	0.1
n-butane	3.7×10^{-11}	1.1×10^{-9}	3.4	4.8×10^{-12}	1.1×10^{-9}	0.5
n-pentane	2.5×10^{-10}	1.1×10^{-9}	23	5.9×10^{-11}	1.1×10^{-9}	5.4
n-hexane	3.0×10^{-10}	1.1×10^{-9}	27	2.0×10^{-10}	1.1×10^{-9}	17
n-heptane	3.4×10^{-10}	1.2×10^{-9}	29	2.6×10^{-10}	1.2×10^{-9}	22

[a] The rate constant has units of cm^3 molecule^{-1} s^{-1}.

TABLE 3: Percentage Abundance of Primary Products Observed in the Reactions of $FeCF_3^+$ and $CoCF_3^+$ with Various Alkenes

	$FeCF_3^+$			$CoCF_3^+$		
alkanes	neutral lost	products	%	neutral lost	products	%
C_2H_4	CF_2	$FeF(C_2H_4)^+$	100	CF_2	$CoF(C_2H_4)^+$	100
C_3H_6	CF_2	$FeF(C_3H_6)^+$	100	CF_2	$CoF(C_3H_6)^+$	92
				CF_3H	$Co(C_3H_5)^+$	8
1-C_4H_8	CF_2	$FeF(C_4H_8)^+$	100	CF_2	$CoF(C_4H_8)^+$	93
				CF_3H	$Co(C_4H_7)^+$	7
i-C_4H_8	CF_2	$FeF(C_4H_8)^+$	100	CF_2	$CoF(C_4H_8)^+$	94
				CF_3H	$Co(C_4H_7)^+$	6
cis-2-C_4H_8	CF_2	$FeF(C_4H_8)^+$	100	CF_2	$CoF(C_4H_8)^+$	100
1,3-C_4H_6	CF_2	$FeF(C_4H_6)^+$	100	CF_2	$CoF(C_4H_6)^+$	100

between Fe^+ and CF_3, the interaction has a substantial electrostatic component, as evidenced by the long bond distance and charge distribution. The calculated bond dissociation energy of Fe^+-CF_3 is 41.4 kcal/mol, which can be compared to $D^0(Fe^+\text{-}CH_3) = 65 \pm 5$ kcal/mol.[59] It is evident that the bond dissociation energy is decreased upon fluorine substitution on methyl radical.

Along the reaction coordinate, a C−F insertion species **2** is located, which is 37.3 kcal/mol more stable than the original entrance channel and lies 4.1 kcal/mol above complex **1**. Complex **2** has C_{2v} symmetry with a slightly distorted CF_2 group binding to Fe through carbon at a distance of 1.977 Å. R(C−F) and ∠FCF are calculated as 1.273 Å and 111.0°, respectively, compared to 1.308 Å and 104.6° for uncomplexed CF_2 in its ground state.[60] The third F bounds to Fe at a distance of 1.724 Å covalently, given that r(Fe−F) is normally at 1.72 Å.[61] The saddle point $TS_{1\rightarrow2}$ (a quintuplet state with C_s symmetry) between **1** and **2** is found to be 35.0 kcal/mol below the entrance channel. Thus, the activation barrier for **1** → **2** conversion is 6.4 kcal/mol with respect to complex **1**. This transition structure is characterized by an imaginary frequency, 250.4i cm^{-1}, which corresponds to C−F bond insertion and formation of a C−F−Fe bridging structure. Compared to the structure of complex **1**, the Fe−C distance is shortened by 0.057 Å. Also, the Fe−F bond length of 1.999 Å for $TS_{1\rightarrow2}$ is elongated compared to that of complex **2**. The corresponding triplet $TS_{1\rightarrow2}$ is less stable by 14.0 kcal/mol.

The next minimum structure on the potential energy surface is structure **3**, which is the true global minimum and is found to be 44.6 kcal/mol below the entrance channel. As shown in Figure 6, the optimized structure is almost planar with a Fe−F bond length of 1.727 Å and a CF_2 unit bound to Fe electrostatically through one F atom by a distance of 1.972 Å. The CF_2 unit is distorted with one C−F bond length elongated to 1.601 Å and the other C−F bond shortened to 1.217 Å, compared to the value of 1.308 Å in free CF_2.[60] The CF_2 subunit binds to FeF^+ primarily by electrostatic interaction. The binding energy

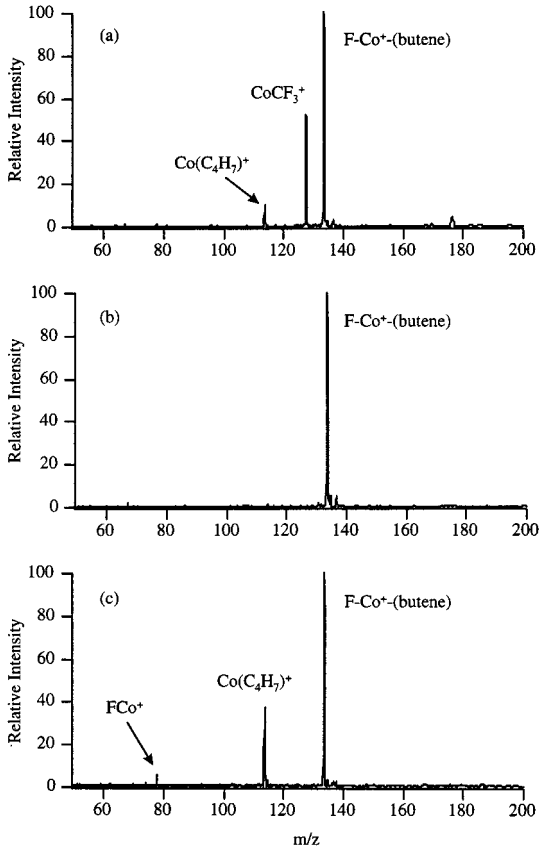

Figure 4. (a) Reaction of $CoCF_3^+$ with 2-methylpropene that was pulsed into the cell at a maximum pressure of ~1.0×10^{-6} Torr, 200 ms; (b) Isolation of product ion, $FCo(butene)^+$; (c) CID of $FCo(butene)^+$. Duration of the excitation RF pulse is 300 μs followed by a 50 ms time delay.

of FFe^+-F_2C is calculated at 34.3 kcal/mol, which is consistent with our experimentally estimated upper limit of 34 ± 2 kcal/mol.

Structures **2** and **3** are connected by a saddle point, $TS_{2\rightarrow3}$ (quintuplet), which is 34.9 kcal/mol below the entrance channel. The relative energies of $TS_{2\rightarrow3}$ with respect to structures **2** and **3** are 2.4 and 9.7 kcal/mol, respectively. The transition-state structure is almost planar. Compared to structure **2**, the Fe−C distance increases significantly, and the CF_2 unit rotates with one F atom pointing at Fe by a distance of 2.089 Å. In addition the C−F bond length is elongated to 1.446 Å, while the other C−F bond is decreased to 1.229 Å. The third F atom is bound to Fe with a bond length of 1.723 Å. The imaginary frequency for this transition state is 220.9i cm^{-1}. The corresponding triplet $TS_{2\rightarrow3}$ is found to be less stable than the quintuplet by 5.4 kcal/mol.

The exit channel is $FFe^+(^5\Sigma) + CF_2$, which is exothermic by 10.3 kcal/mol relative to the entrance channel. The three minima lie close to each other with a maximum energy

TABLE 4: Pseudo-First-Order Rate Constants and Calculated Reaction Efficiencies for the Reactions of $FeCF_3^+$ and $CoCF_3^+$ with Alkenes[a]

	$FeCF_3^+$			$CoCF_3^+$		
reagent	k_{obs}	k_L	reaction efficiency (%)	k_{obs}	k_L	reaction efficiency (%)
ethylene	5.8×10^{-12}	1.0×10^{-9}	0.6	1.2×10^{-12}	1.0×10^{-9}	0.1
propene	1.2×10^{-11}	1.1×10^{-9}	1.1	2.3×10^{-12}	1.1×10^{-9}	0.2
1-butene	1.6×10^{-11}	1.1×10^{-9}	1.5	2.7×10^{-12}	1.1×10^{-9}	0.3

[a] The rate constant has units of cm^3 molecule^{-1} s^{-1}.

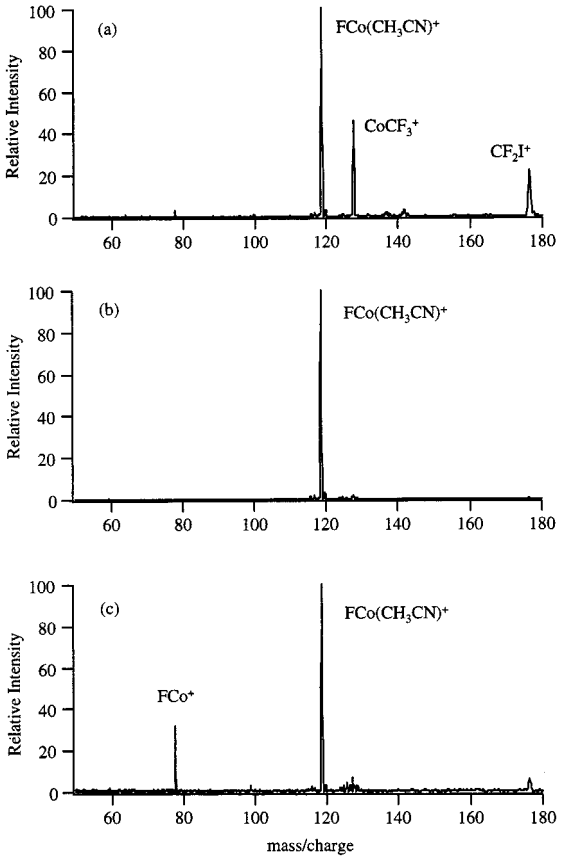

Figure 5. (a) Reaction of $CoCF_3^+$ with acetonitrile that was pulsed into the cell at a maximum pressure of $\sim 1.0 \times 10^{-6}$ Torr, 200 ms; (b) Isolation of product ion, $FCo(CH_3CN)^+$; (c) CID of $FCo(CH_3CN)^+$. Duration of the excitation RF pulse is 300 μs followed by a 50 ms time delay. The peak (*m*/*z* 177), corresponding to CF_2I^+, is from the primary reaction of Co^+ with CF_3I.

separation of only 7.3 kcal/mol. Overall on the potential energy surface, $TS_{1\rightarrow2}$ shows the larger activation barrier (6.4 kcal/mol), which involves C−F activation, and $TS_{2\rightarrow3}$ corresponding to the CF_2 unit rotation has only a 2.4 kcal/mol barrier.

The calculations for $CoCF_3^+$ also yield three similar local minima, as shown in Figure 8. The $^4A''$ ground state of the intact $Co(CF_3)^+$ complex **4** has C_{3v} symmetry and is found to be 39.1 kcal/mol below the entrance channel of $Co^+(^3F) + CF_3^\bullet$. The CF_3 unit remains nearly undisturbed with a C−F bond length of 1.329 Å, an F−C−F bond angle of 110.4°, and a Co−C bond length of 1.989 Å. The corresponding $^2A''$ state of **4** is less stable than the $^4A''$ state by 15.6 kcal/mol. $D^0(Co^+-CF_3)$ is calculated at 39.1 kcal/mol, compared to $D^0(Co^+-CH_3) = 57 \pm 7$ kcal/mol.[59] The $^4A''$ ground state of the inserted $F-Co^+-CF_2$ complex **5** is 33.0 kcal/mol more stable than the entrance channel. Its corresponding $^2A''$ state is less stable by 30.0 kcal/mol. The inserted complex has C_{2v} symmetry with a Co−C distance of 2.025 Å and a Co−F distance of 1.724 Å. The C−F bond length in the CF_2 unit is slightly shortened. The global minimum structure of

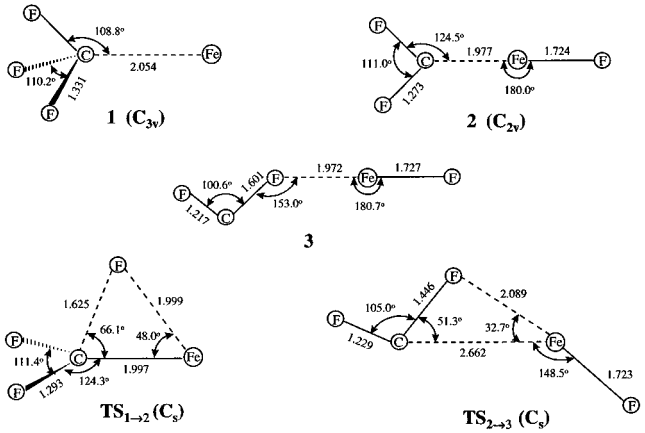

Figure 6. Optimized geometries of structures **1**, **2**, and **3**, and the transition−state structures $TS_{1\rightarrow2}$ and $TS_{2\rightarrow3}$ for the $Fe(CF_3)^+$ complex. The units of bond lengths and bond angles are Å and deg, respectively.

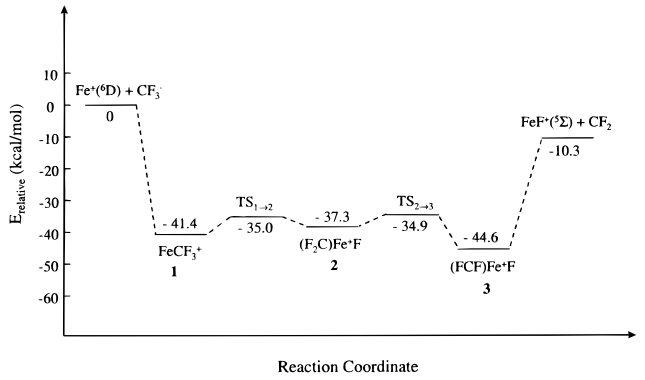

Figure 7. Potential energy surface diagram of the [Fe, C, F_3]$^+$ system.

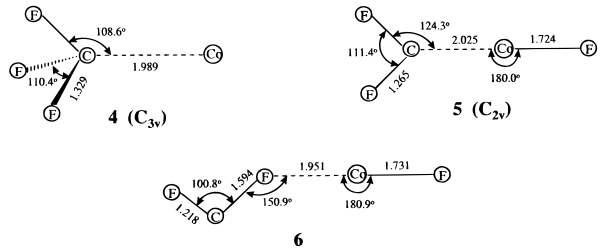

Figure 8. Optimized geometries of structures **4**, **5**, and **6** for the $Co(CF_3)^+$ complex. The units of bond lengths and bond angles are Å and deg, respectively.

(FCF)···Co^+−F ion-dipole complex **6** lies 42.9 kcal/mol below the entrance channel, and 35.7 kcal/mol below the exit channel of $FCo^+(^4\Sigma) + CF_2$, which is exothermic by 7.2 kcal/mol relative to the entrance channel. The optimized quadruplet structure is almost planar, and the structural details are shown in Figure 8. The corresponding doublet is less stable by 22.1 kcal/mol. $D^0(FCo^+-F_2C)$ is calculated to be 35.7 kcal/mol, which is somewhat higher than our rough experimentally estimated upper limit of 30.9 ± 1.4 kcal/mol. The transition-

state structures were not determined for the $Co(CF_3)^+$ complex. However, we assume that they are similar to those of the [Fe, C, F_3]$^+$ system. Both $FeCF_3^+$ and $CoCF_3^+$ undergo similar C−F activation mechanisms. Furthermore, in a previous study on the potential energy surface of the [Ni, C, F_3]$^+$ system, we observed an analogous C−F bond activation in which initial C−F activation takes place with a large activation barrier of 13.6 kcal/mol, followed by rotation of the CF_2 group to the final (FCF)···Ni^+−F structure with an activation barrier of 11.1 kcal/mol.[62]

8. Associated Thermochemistry. We can compare the calculated energetics in this work to other determined literature values. If the theoretical value of $D^0(Fe^+-F) = 101$ kcal/mol is used,[27] together with $\Delta H_f(F) = 19.0 \pm 0.1$ kcal/mol,[63] $\Delta H_f(CF_2) = -49 \pm 3$ kcal/mol,[63] and $\Delta H_f(CF_3) = -110$ kcal/mol,[63] $\Delta H_{rxn}(13)$ is determined to be -21 ± 6 kcal/mol from eq 14. This value is in fair agreement with our calculated value of −10.3 kcal/mol, indicating an exothermic reaction.

$$Fe^+ + CF_3 \rightarrow FeF^+ + CF_2 \quad (13)$$

$$\Delta H_{rxn}(13) = \Delta H_f(F) + \Delta H_f(CF_2) - D^0(Fe^+-F) - \Delta H_f(CF_3) \quad (14)$$

$$Fe^+ + CF_3I \rightarrow FeCF_3^+ + I \quad (15)$$

$$\Delta H_{rxn}(15) = \Delta H_f(F) + \Delta H_f(CF_2) + \Delta H_f(I) - D^0(Fe^+-F) - D^0(FeF^+-F_2C) - \Delta H_f(CF_3I) \quad (16)$$

Similarly, if the calculated $D^0(FeF^+-F_2C) = 34.3$ kcal/mol is used for the most stable $FeCF_3^+$ structure, together with $D^0(Fe^+-F) = 101$ kcal/mol,[27] $\Delta H_f(CF_3I) = -141 \pm 5$ kcal/mol,[63] $\Delta H_f(CF_2) = -49 \pm 3$ kcal/mol,[63] $\Delta H_f(F) = 19.0 \pm 0.1$ kcal/mol,[63] and $\Delta H_f(I) = 25.5$ kcal/mol,[63] $\Delta H_{rxn}(15)$ is estimated to be 1.2 ± 9 kcal/mol from eq 16. Similar thermochemistry considerations can be applied to reactions 17 and 18. If the theoretical value of $D^0(Co^+-F) = 91.9$ kcal/mol is used,[64] $\Delta H_{rxn}(17)$ is determined to be -11.9 ± 6 kcal/mol from eq 19, which is in good agreement with our calculated −7.2 kcal/mol, indicating an exothermic reaction. On the basis of the same thermochemistry data and the calculated bond energies, ΔH_{rxn}(18) is estimated to be 8.9 ± 9 kcal/mol from eq 20. The fact that both $FeCF_3^+$ and $CoCF_3^+$ can readily be formed, however, suggests that reactions 15 and 18 are near thermoneutral or slightly exothermic.

$$Co^+ + CF_3 \rightarrow CoF^+ + CF_2 \quad (17)$$

$$Co^+ + CF_3I \rightarrow CoCF_3^+ + I \quad (18)$$

$$\Delta H_{rxn}(17) = \Delta H_f(F) + \Delta H_f(CF_2) - D^0(Co^+\text{-}F) - \Delta H_f(CF_3) \quad (19)$$

$$\Delta H_{rxn}(18) = \Delta H_f(F) + \Delta H_f(CF_2) + \Delta H_f(I) - D^0(Co^+-F) - D^0(CoF^+-F_2C) - \Delta H_f(CF_3I) \quad (20)$$

Conclusions

The gas-phase reactions of MCF_3^+ (M = Fe, Co) with small hydrocarbons and other reagents such as benzene, acetonitrile and water, as well as collision-induced dissociation (CID), reveal that the structure of MCF_3^+ corresponds to a [FM^+···F_2C] ion−dipole complex. Interestingly, CF_2 loss in the EI spectra of cerium chelates containing the CF_3 group has been reported.[65] It is proposed to form by a mechanism involving cleavage of the Ce−CF_3 bond, migration of fluorine atom to the metal, and formation of metal−F bonds.[65,66] Paulino and Squires have reported an analogous finding for CF_2Cl^-, which corresponds to a carbene−halide anion structure consisting of a free carbene moiety bound electrostatically through carbon to Cl^-, with nearly a full −1 charge on Cl atom.[67,68] Recent theoretical calculations by Schleyer and co-workers have shown that AH_3^+ is actually HA^+···H_2 for A = Sn and Pb, while CH_3^+ and SiH_3^+ are strongly bound D_{3h} structures.[69] The predominant electrostatic bonding between FM^+ and CF_2 leads to dominant CF_2 displacement reactions for various reagents. Pseudo-first-order kinetics are observed for the reactions of MCF_3^+ with small hydrocarbons. The reaction rates between MCF_3^+ and alkane increase dramatically as the alkane chain length increases. Ion−molecule reactions and competitive CID yield 17.9 ± 1.0 kcal/mol $< D^0(FFe^+-F_2C) < 34 \pm 2$ kcal/mol, and $D^0(FCo^+-F_2C) < 30.9 \pm 1.4$ kcal/mol.

Density functional calculations provide further insight on the C−F activation mechanism. Geometries and energetics of local minima for the [Fe, C, F_3]$^+$ and [Co, C, F_3]$^+$ complexes were obtained. For the [Fe, C, F_3]$^+$ system, three local minima and two transition structures are found on the potential energy surface. Initially, an intact Fe^+−CF_3 complex is formed, which goes on to an inserted fluoro-difluorocarbene F_2C−Fe^+−F isomer. A transition structure connecting these two local minima indicates an activation barrier of 6.4 kcal/mol for the C−F activation process. From the inserted structure to the global minimum structure of FCF···Fe^+−F, there is only a small activation barrier. This unique C−F activation mechanism is also expected to apply to the [Co, C, F_3]$^+$ complex, since similar local minina are found on its potential energy surface. The calculated bond energies of FM^+−F_2C are 34.3 and 35.7 kcal/mol for M = Fe and Co, respectively, which are in general agreement with the experimental results.

Acknowledgement is made to the Division of Chemical Sciences in the Office of Basic Energy Sciences in the U.S. Department of Energy (under Grant DE-FG02-87ER13766) and the National Science Foundation (CHE-9627221). The authors thank Professor Einar Uggerud at the Department of Chemistry, University of Oslo, Norway, and Dr. Charles W. Bauschlicher, Jr., at NASA Ames Research Center, Moffett Field, for inspiring discussions. The authors also thank Professor Sabre Kais at the Department of Chemistry, Purdue University, for essential help on theoretical calculations.

References and Notes

(1) (a) Russell, D. H. Ed. *Gas-Phase Inorganic Chemistry*; Plenum Press: New York, 1989. (b) Eller, K.; Schwarz, H. *Chem. Rev.* **1991**, *91*, 1121. (c) Freiser, B. S. *Acc. Chem. Res.* **1994**, *27*, 353. (d) van Koppen, P. A. M.; Bowers, M. T.; Fisher, E. R.; Armentrout, P. B. *J. Am. Chem. Soc.* **1994**, *116*, 3780. (e) Freiser, B. S., Ed. *Organometallic Ion Chemistry*; Kluwer Academic Publishers: Dordrecht, 1996. (f) Freiser, B. S. *J. Mass Spectrom.* **1996**, *31*, 703.

(2) Allison, J.; Freas, R. B.; Ridge, D. P. *J. Am. Chem. Soc.* **1979**, *101*, 1332.

(3) Jacobson, D. B.; Freiser, B. S. *J. Am. Chem. Soc.* **1983**, *105*, 5197.

(4) Halle, L. F.; Houriet, R.; Kappes, M. M.; Stanley, R. H.; Beauchamp, J. L. *J. Am. Chem. Soc.* **1982**, *104*, 6293.

(5) Georgiadis, R.; Fisher, E. R.; Armentrout, P. B. *J. Am. Chem. Soc.* **1989**, *111*, 4251.

(6) Freas, R. B.; Ridge, D. P. *J. Am. Chem. Soc.* **1980**, *102*, 7129.

(7) (a)Jacobson, D. B.; Freiser, B. S. *J. Am. Chem. Soc.* **1984**, *106*, 3891. (b) Jacobson, D. B.; Freiser, B. S. *J. Am. Chem. Soc.* **1985**, *107*, 5876.

(8) Jackson, T. C.; Jacobson, D. B.; Freiser, B. S. *J. Am. Chem. Soc.* **1984**, *106*, 1252.

(9) (a) Schröder, D.; Schwarz, H. *Angew. Chem., Int. Ed. Engl*. **1990**, *29*, 1443. (b) Shaik, S.; Danovich, D.; Fiedler, A.; Schröder, D.; Schwarz, H. *Helv. Chim. Acta* **1995**, *78*, 1393. (c) Schröder, D.; Wesendrup, R.; Schalley, C. A.; Zummack, W.; Schwarz, H. *Helv. Chim. Acta.* **1996**, *79*, 123.

(10) (a) Clemmer, D. E.; Aristov, N.; Armentrout, P. B. *J. Phys. Chem*. **1993**, *97*, 544. (b) Clemmer, D. E.; Chen, Y.-M.; Khan, F. A.; Armentrout, P. B. *J. Phys. Chem*. **1994**, *98*, 6522. (c) Chen, Y.-M.; Clemmer, D. E.; Armentrout, P. B. *J. Am. Chem. Soc.* **1994**, *116*, 7815.

(11) Jackson, T. C.; Carlin T. J.; Freiser, B. S. *Int. J. Mass Spectrom. Ion Processes* **1986**, *72*, 169.

(12) Allison, J. *Inorg. Chem.* **1986**, *34*, 627.

(13) Ravishankara, A. R.; Turnipseed, A. A.; Jensen, N. R.; Barone, S.; Mills, M.; Howard, C. J.; Solomon, S. *Science* **1994**, *263*, 72.

(14) Wallington, T. J.; Schneider, W. F.; Worsnop, D. R.; Nielsen, O. J.; Sehested, J.; Debruyn, W. J.; Shorter, J. A. *Environ. Sci. Technol.* **1994**, *28*, 320A.

(15) Brahms, D. L. S.; Dailey, W. P. *Chem. Rev.* **1996**, *96*, 1585.

(16) Dolbier, W. R. *Chem. Rev.* **1996**, *96*,1557.

(17) Halle, L. F.; Armentrout, P. B.; Beauchamp, J. L. *Organometallics* **1983**, *2*, 1829.

(18) (a) Harrison, R. G.; Richmond, T. G. *J. Am. Chem. Soc*. **1993**, *115*, 5303. (b) Kiplinger, J. L.; Richmond, T. G.; Osterberg, C. E. *Chem. Rev.* **1994**, *94*, 373.

(19) Burns, C. J.; Andersen, R. A. *J. Chem. Soc., Chem. Commun.* **1989**, 136.

(20) (a) Aizenberg, M.; Milstein, D. *Science* **1994**, *265*, 359. (b) Aizenberg, M.; Milstein, D. *J. Am. Chem. Soc.* **1995**, *117*, 8674.

(21) (a) Burdeniuc, J.; Crabtree, R. H. *J. Am. Chem. Soc.* **1996**, *118*, 2525. (b) Burdeniuc, J.; Crabtree, R. H. *Science* **1996**, *271*, 340.

(22) (a) Pradeep, T.; Ast, T.; Cooks, R. G.; Feng, B. *J. Phys. Chem.* **1994**, *98*, 9301. (b) Pradeep, T.; Riederer, D. E. Jr.; Hoke, II, S. H.; Cooks, R. G.; Linford, M. R. *J. Am. Chem. Soc.* **1994**, *116*, 8658.

(23) Dietz, T. G.; Chatellier, D. S.; Ridge, D. P. *J. Am. Chem. Soc.* **1978**, *100*, 4905.

(24) Bjarnason, A,; Taylor, J. W. *Organometallics* **1989**, *8*, 2020.

(25) Chen, G.; Hoke, II, S. H.; Cooks, R. G. *Int. J. Mass Spectrom. Ion Processes* **1994**, *139*, 87.

(26) Garciá, E.; Huang, Y.; Freiser, B. S. *Inorg. Chem.* **1993**, *32*, 3595.

(27) Schröder, D.; Hru?ák, J.; Schwarz, H. *Helv. Chim. Acta* **1992**, *75*, 2215.

(28) Cornehl, H. H.; Hornung, G.; Schwarz, H. *J. Am. Chem. Soc.* **1996**, *118*, 9960.

(29) Harvey, J. N.; Schröder, D.; Koch, W.; Danovich, D.; Shaik, S.; Schwarz, H. *Chem. Phys. Lett.* **1997**, *273*, 164.

(30) Chen, Q.; Lin, C. -Y.; Chen, H.; Freiser, B. S. *Organometallics* **1997**, *16*, 4020.

(31) Freiser, B. S. *Talanta* **1985**, *32*, 697.

(32) Cody, R. B.; Burnier, R. C.; Reents, W. D., Jr.; Carlin, T. J.; McCrery, D. A.; Lengel, R. K.; Freiser, B. S. *Int. J. Mass Spectrom. Ion Processes* **1980**, *33*, 37.

(33) (a) Cooks, R. G., Ed. *Collision Spectroscopy*; Plenum: New York, 1978. (b) Burnier, R. C.; Cody, R. B.; Freiser, B. S. *J. Am. Chem. Soc.* **1982**, *104*, 7436.

(34) Gauthier, J. W.; Trautman, T. R.; Jacobson, D. B. *Anal. Chim. Acta* **1991**, *246*, 211.

(35) Allison, J.; Ridge, D. P. *J. Am. Chem. Soc.* **1979**, *101*, 4998.

(36) Carlin, T. J.; Freiser, B. S. *Anal. Chem.* **1983**, *55*, 571.

(37) Comisarow, M. B.; Grassi, V.; Parisod, G. *Chem. Phys. Lett.* **1978**, *57*, 413.

(38) (a) Freiser, B. S. In *Techniques for the Study of Ion Molecule Reactions*; Farrar, J. M., Saunders, W. H., Eds.; Wiley: New York, 1988; p 61. (b) Grosshans, P. B.; Marshall, A. G. *Anal. Chem.* **1991**, *63*, 2057.

(39) Bartmess, J. E.; Georgiadis, R. M. *Vacuum* **1983**, *33*, 149.

(40) (a) Becke, A. D. *Phys. Rev.* **1988**, *A38*, 3098. (b) Becke, A. D. *J. Chem. Phys.* **1993**, *98*, 1372. (c) Becke, A. D. *J. Chem. Phys*. **1993**, *98*, 5648. (d) Stephens, P. J.; Devlin, F. J.; Chabalowski, C. F.; Frisch, M. J. *J. Phys. Chem.* **1994**, *98*, 11623.

(41) Kais, S.; Herschbach, N. C. H.; Murray, C. W.; Lamimg, G. J. *J. Chem. Phys.* **1993**, *99*, 417.

(42) Siegbahn, P. E. M. *Adv. Chem. Phys.* **1996**, *XCIII*, 333.

(43) (a) Wachters, A. J. H. *J. Chem. Phys.* **1970**, *52*, 103. (b) Hay, P. J. *J. Chem. Phys.* **1977**, *66*, 4377.

(44) Bauschlicher, Jr., C. W. *Chem Phys. Lett.* **1995**, *246*, 40.

(45) Fiedler, A.; Schröder, D.; Schwarz, H.; Tjelta, B. L.; Armentrout, P. B. *J. Am. Chem. Soc.* **1996**, *118*, 5047.

(46) Frisch, M. J.; Trucks, G. W.; Schlegel, H. B.; Gill, P. M. W.; Johnson, B. G.; Robb, M. A.; Cheeseman, J. R.; Keith, T. A.; Petersson, G. A.; Montgomery, J. A.; Raghavachari, K.; Al-Laham, M. A.; Zakrzewski, V. G.; Ortiz, J. V.; Foresman, J. B.; Cioslowski, J.; Stefanov, B. B.; Nanayakkara, A.; Challacombe, M.; Peng, C. W.; Ayala, P. Y.; Chen, W.; Wong, M. W.; Anfres, J. L.; Replogle, E. S.; Gomperts, R.; Martin, R. L.; Fox, D. J.; Binkley, J. S.; Defrees, D. J.; Baker, J.; Stewart, J. P.; Head-Gordon, M.; Gonzalez, C.; Pople, J. A. *Gaussian 94* (Revision D.1); Gaussian, Inc.: Pittsburgh PA, 1995.

(47) Schultz, R. H.; Armentrout, P. B. *J. Am. Chem. Soc.* **1991**, *113*, 729.

(48) Armentrout, P. B.; Kickel, B. L. In *Organometallic Ion Chemistry*; Freiser, B. S., Ed.; Kluwer Academic Publishers: Dordrecht, 1996; Chapter 1.

(49) Su, T.; Bowers, M. T. In *Gas Phase Ion Chemistry*; Bowers, M. T., Ed.; Academic Press: New York, 1979; Vol. 1, p 83.

(50) Jacobson, D. B.; Freiser, B. S. *J. Am. Chem. Soc.* **1983**, *105*, 7484.

(51) Labanowski, J. K.; Andzelm, J. W. *Density Functional Methods in Chemistry*; Springer-Verlag: New York, 1991.

(52) Bauschlicher, C. W., Jr.; Patridge, H. *Chem Phys. Lett.* **1995**, *240*, 533.

(53) Ricca, A.; Bauschlicher, C. W., Jr. *Chem Phys. Lett.* **1995**, *245*, 150.

(54) Heinemann, C.; Hertwig, R. H.; Wesendrup, R.; Koch, W.; Schwarz, H. *J. Am. Chem. Soc.* **1995**, *117*, 495.

(55) Holthausen, M. C.; Fiedler, A.; Schwarz, H.; Koch, W. *J. Phys. Chem.* **1996**, *100*, 6236.

(56) Holthausen, M. C.; Koch, W. *J. Am. Chem. Soc.* **1996**, *118*, 9932.

(57) Geometry of ground-state free CF_3 radical with Becke3LYP/6-311+G*: R(C−F) = 1.323 Å, ∠F−C−F = 111.3°.

(58) Bauschlicher, C. W., Jr.; Langhoff, S. R.; Partridge, H.; Barnes, L. A. *J. Chem. Phys.* **1989**, *91*, 2399.

(59) Hettich, R. L.; Jackson, T. C.; Stanko, E. M.; Freiser, B. S. *J. Am. Soc. Chem.* **1986**, *108*, 5086.

(60) Geometry of ground-state free CF_2 with Becke3LYP/6-311+G*: R(C−F) = 1.308 Å, ∠F−C−F = 104.6°.

(61) Becke3LYP of ground-state FeF^+ with 6-311+G* for F and Wachters−Hay all-electron basis set for Fe: R(Fe−F) = 1.720 Å. At this level of theory, $D^0(Fe^+-F)$ is calculated as 92.3 kcal/mol, which is in good agreement with the experimental value of 93.5 ± 7.5 kcal/mol (ref 27).

(62) Chen, Q.; Freiser, B. S. *Chem. Phys. Lett.*, in press.

(63) Lias, S. G.; Bartmess, J. E.; Liebman, J. F.; Holmes, J. L.; Levin, R. D.; Mallard, W. G. Gas-Phase Ion and Neutral Thermochemistry. *J. Phys. Chem. Ref. Data* **1988**, *17*, Suppl. 1.

(64) $D^0(Co^+-F)$ is calculated as 91.9 kcal/mol using Becke3LYP with 6-311+G* for F and Wachters−Hay all-electron basis set for Co.

(65) Schildcrout, S. M. *Inorg. Chem.* **1985**, *24*, 760.

(66) (a) Bancroft, G. M.; Reichert, C.; Westmore, J. B. Gesser, H. D. *Inorg. Chem.* **1969**, *8*, 474. (b) Clobes, A. L.; Morris, M. L.; Koob, R. D. *Org. Mass Spectrom.* **1971**, *5*, 633.

(67) Paulino, J. A.; Squires, R. R. *J. Am. Chem. Soc.* **1991**, *113*, 1845.

(68) Paulino, J. A.; Squires, R. R. *J. Am. Chem. Soc.* **1991**, *113*, 5573.

(69) Kapp, J.; Schreiner, P. R.; Schleyer, P. V. R. *J. Am. Chem. Soc.* **1996**, *118*, 12154.